Physiological Features of the S- and M-cone Photoreceptors of Wild-type Mice from Single-cell Recordings

Sergei S. Nikonov,[1] Roman Kholodenko,[1,2] Janis Lem,[3] and Edward N. Pugh Jr.[1]

[1]F.M. Kirby Center for Molecular Ophthalmology, Department of Ophthalmology, School of Medicine, University of Pennsylvania, Philadelphia, PA 19104

[2]Chemyakin and Ovchinnikov Institute of Bioorganic Chemistry, Moscow, Russia

[3]Department of Medicine, Department of Ophthalmology, Department of Genetics, Department of Neuroscience, and Program in Cell, Molecular, and Developmental Biology, Tufts-New England Medical Centers, Boston, MA 02111

Cone cells constitute only 3% of the photoreceptors of the wild-type (WT) mouse. While mouse rods have been thoroughly investigated with suction pipette recordings of their outer segment membrane currents, to date no recordings from WT cones have been published, likely because of the rarity of cones and the fragility of their outer segments. Recently, we characterized the photoreceptors of $Nrl^{-/-}$ mice, using suction pipette recordings from their "inner segments" (perinuclear region), and found them to be cones. Here we report the use of this same method to record for the first time the responses of single cones of WT mice, and of mice lacking the α-subunit of the G-protein transducin ($G_t\alpha^{-/-}$), a loss that renders them functionally rodless. Most cones were found to functionally co-express both S- (λ_{max} = 360 nm) and M- (λ_{max} = 508 nm) cone opsins and to be maximally sensitive at 360 nm ("S-cones"); nonetheless, all cones from the dorsal retina were found to be maximally sensitive at 508 nm ("M-cones"). The dim-flash response kinetics and absolute sensitivity of S- and M-cones were very similar and not dependent on which of the coexpressed cone opsins drove transduction; the time to peak of the dim-flash response was ∼70 ms, and ∼0.2% of the circulating current was suppressed per photoisomerization. Amplification in WT cones (A ∼4 s^{-2}) was found to be about twofold lower than in rods (A ∼8 s^{-2}). Mouse M-cones maintained their circulating current at very nearly the dark adapted level even when >90% of their M-opsin was bleached. S-cones were less tolerant to bleached S-opsin than M-cones to bleached M-opsin, but still far more tolerant than mouse rods to bleached rhodopsin, which exhibit persistent suppression of nearly 50% of their circulating current following a 20% bleach. Thus, the three types of mouse opsin appear distinctive in the degree to which their bleached, unregenerated opsins generate "dark light."

The Journal of General Physiology

INTRODUCTION

Healthy cone photoreceptor function is essential to normal human vision for many reasons, including the following. First, cones provide the basis of daytime vision by dint of their ability to maintain their cyclic nucleotide-gated channels (CNGs) open in the presence of illumination that bleaches very high fractions of their pigment (Burkhardt, 1994; Paupoo et al., 2000), an ability involving a number of distinctive molecular and physiological factors that remain only partially understood (Pugh et al., 1999; Rebrik and Korenbrot, 2004). Second, cones generate the signals for color vision by virtue of their diverse spectral sensitivities and their spectrally "opponent" retinal connections (Dacey, 1996, 2000). Third, cones initiate vision in the macula, the highly specialized central region of the retina that maps to a large fraction of human primary visual cortex (Engel et al., 1997). Because of the roles that cone photoreceptors play in normal human vision, cone disease and cell death, as occurs in age-related macular degeneration, the leading cause of blindness in aging humans (Klein et al., 2002), is devastating. To investigate the molecular mechanisms that allow cones to perform their unique functions, and the molecular mechanisms of cone disease, it is critical to have mammalian models which allow (a) genomic analysis and manipulation of genes expressed specifically in cones, (b) molecular and biochemical characterization of the protein products of such genes, and (c) electrophysiological analysis of cones and their neural circuits.

The mouse is the mammal of choice for the investigation of organ function and the molecular mechanisms of disease. There are many reasons for this choice, including the genomic proximity of mice to humans, the large and rapidly growing array of molecular biological tools for targeted gene manipulations in mice, the large knowledge base of molecular, cellular, and behavioral experimentation using mice, and the relatively short generation time and economics of mouse husbandry. Nonetheless for these compelling reasons, the investigation of the

Correspondence to Edward N. Pugh Jr.: pugh@mail.med.upenn.edu

Abbreviations used in this paper: CNG, cyclic nucleotide-gated channels; PDE, phosphodiesterase; WT, wild-type.

functional consequences of molecularly manipulated cone-specific genes in mice has been an elusive goal, having only been achieved in a few studies using electroretinographic methods (Lyubarsky et al., 2000, 2001; Pennesi et al., 2003a,b). In contrast, while recordings from individual mouse rods (most with targeted gene manipulations) have been presented in at least 35 primary publications since the report by Chen et al. (1995), not a single paper has yet been published describing single-cell recordings from WT mouse cones. We believe this defect to arise from a number of factors, including (a) the 30-fold numerical dominance of rods over cones in mouse retina (Carter-Dawson and LaVail, 1979), (b) the lack of morphological features distinguishing cones from rods in mouse retinal slices viewed under the infrared illumination requisite for single-cell recording, and (c) the relative lability of cone vs. rod outer segments removed from their interphotoreceptor matrix sheaths. The latter lability was revealed in experiments with mice lacking the neural retina leucine zipper transcription factor (*Nrl*$^{-/-}$) (Nikonov et al., 2005).

The apparent fragility of *Nrl*$^{-/-}$ outer segments provided the impetus for the development of a novel "loose-patch" method, in which a portion of the photoreceptor circulating current was recorded by drawing the "inner segment" (perinuclear region) of mouse photoreceptors in a retinal slice into a suction pipette (Nikonov et al., 2005). By application of this new method, along with a battery of other analyses, including EM analysis of ultrastructure, quantification of cone-specific proteins, and spectral and kinetic criteria, it was unequivocally established that *Nrl*$^{-/-}$ photoreceptors are a species of cones (Daniele et al., 2005; Nikonov et al., 2005), and not the "cone–rod" (or "cod") intermediates previously supposed (Mears et al., 2001). While the classification of *Nrl*$^{-/-}$ photoreceptors as cones has opened the door to the identification and characterization of many cone-specific genes (Yoshida et al., 2004), questions remain as to the ultimate validity of the *Nrl*$^{-/-}$ retina as model system for the investigation of mouse cone physiology. In part, such questions arise because *Nrl*$^{-/-}$ outer segments exhibit a degree of disorder not present in their WT counterparts, and undergo a slow degeneration that is evident by 6 wk of age (Mears et al., 2001; Daniele et al., 2005). However, a critical question that inevitably arises and must be answered is whether WT mouse cones have functional properties like those of the cones of 4–6-wk-old *Nrl*$^{-/-}$ mice.

Here we address this question and establish that single cone photoreceptors of WT and $G_t\alpha^{-/-}$ mice can be characterized with the suction pipette method previously developed to record stable electrical responses of *Nrl*$^{-/-}$ cones. While most of the physiological features of WT cones determined with this method, including their response kinetics and amplification and their functional coexpression of both S- and M-cone opsins in most cells, are very similar to those of the *Nrl*$^{-/-}$ mouse, one notable difference was found. Thus, there appears to exist in the dorsal retina of the WT mouse a subset of cones that express M-opsin at a higher level than S-opsin. These "M-cones" appear more tolerant to high levels of bleached pigment than the predominant cone type in which the S-opsin is expressed at a higher level. (The mouse genome contains the genes for three opsins expressed in retinal photoreceptors: rhodopsin with λ_{max} = 498 nm, and two cone opsins with λ_{max} = 360 nm and 508 nm, respectively [Yokoyama and Yokoyama, 2000]. As the cone opsin with λ_{max} = 360 nm is a member of the SWS1 family, which also contains the human S-cone opsin, and the cone opsin with λ_{max} = 508 nm is a member of the LWS/MWS family, which contains the human M-cone opsin, throughout this paper we will simply identify the two mouse cone opsins as mouse "S-opsin" and "M-opsin.")

MATERIALS AND METHODS

Animals

All experiments were performed in compliance with National Institutes of Health guidelines, as approved by the Institutional Animal Care and Use Committee of the University of Pennsylvania. Wild-type (WT) mice were C57Bl/6. $G_t\alpha^{-/-}$ mice were generated at the New England Medical Center (Calvert et al., 2000). Animals used for recordings were born and maintained in controlled ambient illumination on a 12 h light/dark cycle, with an illumination level of 2–3 lux, and dark adapted for at least 12 h before experimentation.

Tissue Preparation and Electrophysiological Methods

Mice were killed, the eyes enucleated, and whole retinas removed from eye cups under infra-red illumination. Small pieces of retina were dissected in a drop of chilled Locke's solution (112.5 mM NaCl, 3.6 mM KCl, 2.4 mM $MgCl_2$, 1.2 mM $CaCl_2$, 10 mM HEPES, 0.02 mM EDTA, 20 mM $NaHCO_3$, 3 mM Na_2-succinate, 0.5 mM Na-glutamate, 10 mM glucose), and placed into a recording chamber. The chamber was continuously refreshed with Locke's solution, pH 7.4, equilibrated with 95% O_2 /5% CO_2, and maintained at 35–37°C with a heating system designed for microscopy (ALA Scientific). Using silanized suction pipettes, we recorded from photoreceptors embedded in 50–100-μm diameter slices of retina exclusively in the "OS out" configuration (Nikonov et al., 2005); in this effort several nuclei and conjoined "inner segment" tissue were intentionally drawn into the pipette. Once the tissue was drawn into the pipette, responses were evoked with calibrated flashes of light delivered under control of a customized LabView (National Instruments) interface. The optical system in the configuration used for these experiments has two stimulation channels: the light source in one channel is a tungsten-halogen lamp, and in the second a xenon flash lamp that delivers ~20-μs pulses. Experiments with WT mouse retinal slices required the use of steady illumination to suppress rod activity, and the tungsten-halogen channel was employed for this purpose.

The "inner segment" limb of the rod and cone circulating current is an outward membrane current, carried primarily by K^+ channels; light responses recorded from inner segment membranes are thus recorded by the amplifier as negative-going, resulting from the suppression of the outward membrane current as the cell hyperpolarizes toward the K^+ reversal potential. Here

we will present all photocurrent responses in the conventional manner as positive-going. However, the actual sign (and direction) of the recorded membrane currents will be referred to as needed.

As the expression of mouse M-cone opsin in mice varies in a dorso-ventral gradient (Applebury et al., 2000), we developed a method that allows the dorsal or ventral region of the retina to be dissected under infrared illumination and used for suction pipette recordings (Nikonov et al., 2005). This method has played a critical role in the complete characterization of cone function in the WT mouse.

Light Stimulation and Calibration; WT Mouse Cone Light Collecting Area

The methods of light stimulation and the calibration of flash and step intensities were as previously reported (Nikonov et al., 2005). The number of photoisomerizations Φ per photoreceptor produced by a flash was estimated as the product of the energy density (photons μm^{-2}) and the outer segment light collecting area, a_c (μm^2), calculated with the following formula:

$$a_c = 2.303 f \varepsilon_{max} \gamma C V_{OS} \times 10^{-4}, \quad (1)$$

where f is a factor that depends on the polarization of the incident light relative to the plane of the disc membranes, ε_{max} is the extinction coefficient at the λ_{max} of the pigment in solution, γ the quantum efficiency of photoisomerization, C the concentration (M) of the pigment in the outer segment, and V_{OS} (μm^3) the envelope volume of the outer segment, and the factor 10^{-4} is required for consistency with the dimensions of V_{OS}. We previously summarized these factors in detail and obtained the estimates a_c = 0.5 μm^2 for WT mouse rods and a_c = 0.11 μm^2 for *Nrl*$^{-/-}$ cones for light flashes and steps delivered in our recording chamber at the λ_{max}'s of the three mouse opsins (Nikonov et al., 2005). In a separate investigation (Daniele et al., 2005), we summarized relevant quantitative features of the ultrastructure of the outer segments of *Nrl*$^{-/-}$ cones and of WT mouse cones and rods (Carter-Dawson and LaVail, 1979) that contribute to a_c. In particular, the diameter and length of the WT mouse cone outer segment are 1.2 μm and 13.4 μm, respectively, yielding an envelope volume V_{OS} = 14 μm^3, as compared with V_{OS} = 37 μm^3 for the WT mouse rod. At a standard concentration of 3 mM relative to the envelope volume, a dark adapted mouse cone with V_{OS} = 14 μm^3 comprises a total of $N_{dark} = 2.7 \times 10^7$ opsin molecules. Based on these facts, we thus estimate the transversely stimulated, fully dark-adapted WT mouse cone to have a collecting area a_c = 0.2 μm^2 at the λ_{max} of its dominant opsin. This likely somewhat overestimates a_c of the cones whose results are reported here for three reasons. First, as most cones coexpress both opsins, and as the concentration of total opsin in the outer segment is likely an approximately conserved quantity, the concentration of the principal cone opsin may be reduced somewhat due to coexpression of the second opsin. Second, photoreceptors have evolved to guide light from their inner segments to their outer segments, and cones in particular have inner segments whose tapering and refractive index distribution assist this guiding, and "impedance match" inner and outer segment refractive indices relative to the index of the extracellular space; transverse stimulation, particularly of very thin outer segments, may reduce collection efficiency due to the refractive index mismatch with the extracellular medium. Third, the nearly continuous exposure to the strong 500-nm background light used to suppress rod activity, and the exposure to the still more intense steps and flashes of light required to determine a cone's step response vs. intensity relation, produce substantial bleaching of the M-opsin. To deal with this latter problem, assuming no regeneration occurs, we programmed a (post-hoc) analysis of the data to create a "bleach progress meter" that estimated the fraction of unbleached pigment $p(T)$ remaining at any given time T during an experiment. The rate equation for bleaching of a transversely stimulated photoreceptor can be written

$$\frac{dp}{dt} = \frac{1}{N_{dark}} \frac{dN}{dt} = -\frac{a_C(p) I(t)}{N_{dark}}, \quad (2)$$

where $a_C(p)$ represents the collecting area in μm^2 when a fraction p of pigment ("unbleached opsin") is present, and $I(t)$ is the stimulus intensity expressed in photons $\mu m^{-2} s^{-1}$. By inserting into Eq. 2, the expression for a_C given by Eq. 1 and solving, one obtains

$$p(T) = \exp\left[-(8 \times 10^{-9}) \int_0^T I(t)\,dt\right], \quad (3)$$

where the number 8×10^{-9} comes from the evaluation of Eq. 1 and is the effective cross section (in μm^2) of a single visual pigment molecule in the recording chamber. The effective collecting area of an individual cone at time T in an experiment is given by $a_C(p(T)) = a_{C,dark}\, p(T)$.

Quantitative Analysis of Response Data

The activation phase of families of normalized responses $R(t)$ were fitted with a model of the phototransduction cascade (Lamb and Pugh, 1992; Pugh and Lamb, 1993),

$$R(t) \equiv \frac{r(t)}{r_{max}} = 1 - \exp[-\tfrac{1}{2}\Phi A (t - t_{eff})^2]. \quad (4)$$

In Eq. 4, "≡" signifies a definition, $r(t)$ is the photoresponse, r_{max} its saturating amplitude, Φ the number of photoisomerizations produced by the flash, and t_{eff} a brief (several ms) delay. Traces computed with Eq. 4 were convolved with digital filters to incorporate the effects of the membrane time constants of cones (Smith and Lamb, 1997) (set to τ_m = 5 ms), and the measured impulse response function of the 8-pole analogue Bessel filter, whose bandwidth was set to 20 Hz.

Amplitude vs. intensity functions were derived from flash response families and fitted with hyperbolic saturation functions of the form

$$R_{peak} = \frac{r(t_{peak})}{r_{max}} = \frac{Q}{Q + Q_{1/2}}, \quad (5)$$

where $r(t_{peak})$ is the amplitude at the time to peak, t_{peak}, of the response, r_{max} the saturating response amplitude, Q is the flash intensity in photons μm^{-2}, and $Q_{1/2}$ the half-saturating intensity. With the amplitude–intensity function expressed in these units, the flash sensitivity S_F of the normalized response is $S_F = 1/Q_{1/2}$. We found that the same formal relation could also be applied to the response to steps of light:

$$R_\infty = \frac{r_\infty}{r_{max}} = \frac{I}{I + I_{1/2}}. \quad (6)$$

Here r_∞ is the steady-state response to a light step of intensity I, and $I_{1/2}$ is the intensity that suppresses half the light-sensitive current.

RESULTS

Isolation of Cone Responses from WT Mouse Retinal Slices with 500-nm Background Steps

The nuclei of mouse cones are located at the outermost row of the 11–12 rows of nuclei in the outer nuclear

layer (ONL) of the retina, just "below" the outer limiting membrane (Carter-Dawson and LaVail, 1979). We took advantage of this histological feature to enhance the probability of drawing a cone "inner segment" into the suction pipette (Fig. 1, A–C). Once the suction pipette was positioned nearby the outer layer of the ONL, the experimenter drew nuclei into the pipette, one at a time. Background steps of 500-nm light were applied to suppress the rod current, and superimposed flashes delivered to test for the presence of current arising from a cone (Fig. 1 D). Additional nuclei were drawn in until a flash response was recorded in the presence of a strong background. Several nuclei (up to ~10) were drawn into the pipette to obtain such a response. To determine the background intensity used to suppress rod currents, we measured the step response amplitude vs. intensity relation for the sensitive component of current (Fig. 1 E, colored symbols), and compared this with the step response functions of individual rods (Fig. 1 E, gray symbols). The data can be described by a hyperbolic saturation function (Eq. 6), with parameter $I_{1/2}$, the intensity required to suppress 50% of the circulating current; for these experiments $I_{1/2}$ ~350 photons $\mu m^{-2}s^{-1}$. Given a rod light collecting area a_c = 0.5 μm^2, the corresponding half-saturating photoisomerization rate, 175 s^{-1}, is consistent with previous determinations: in rat rods, 161 s^{-1} (Nakatani et al., 1991); in mouse rods, 250 s^{-1} (Lyubarsky and Pugh, 1996) and 120 s^{-1} (Xu et al., 1997). Based on Eq. 6, and the value $I_{1/2}$ ~350 photons $\mu m^{-2}s^{-1}$, a background of 20,000 photons $\mu m^{-2}s^{-1}$ is predicted to suppress ~98.3% of the circulating current of individual rods. As the typical current recorded by the suction pipette in our experiments was ~40 pA, it follows that the rod current not suppressed by the background should have been <0.7 pA. Nonetheless, in the presence of this background, the suction electrode routinely recorded a residual current of 5–15 pA, which responded only weakly to modest increases in steady background, but which could be suppressed by strong flashes (Fig. 1 D). We concluded that this residual current originated in a single cone cell based on its properties, which we now describe.

Light Responses Recorded from the "Inner Segment" Are Highly Stable

The properties of light responses measured in the presence of the standard 500-nm background of 20,000 photons $\mu m^{-2}s^{-1}$ were stable over recording sessions that lasted up to 1.5 h, and in which 1,000 or more light stimuli were delivered and responses recorded

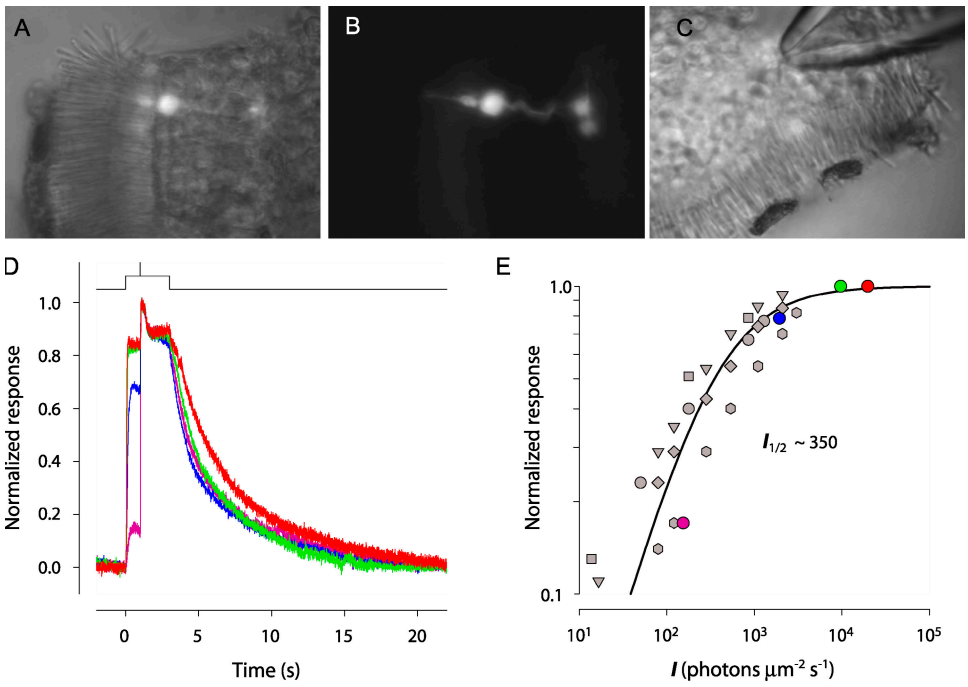

Figure 1. Isolation of WT cone responses. (A) Combined infra-red and fluorescence images of a retinal slice of a mouse expressing EGFP under the human LWS/MWS cone promoter (Fei and Hughes, 2001), as seen in the recording chamber. (B) Fluorescence image alone, revealing details of the cone in A. (C) Infra-red image of another slice illustrating method of drawing several "inner segments" into the suction pipette. (D) Recordings from experiment, as illustrated in C: averaged step responses to 4 different intensities of 500-nm light with superimposed 361-nm flash. At 1 s after step onset, the flash was presented; the step was terminated 2 s later; this timing of the background step and flash were used in all experiments. (E) Amplitudes of step responses from D (colored symbols correspond to colored traces), renormalized by the amplitude of the step response to the most intense step (red trace). Gray symbols are data from individual rods. The smooth curve plots Eq. 6 with $I_{1/2}$ = 350 photons $\mu m^2 s^{-1}$.

(unpublished data). The stability of the saturating amplitude of the photocurrent is particularly noteworthy.

Six Lines of Evidence Establish that the Responses Are Generated by Mouse Cones

Six distinct lines of evidence can be presented at this point in support the conclusion that the photoresponses recorded in the presence of the standard background were generated by WT mouse cones. First, as mentioned above, recordings from rods and calculations with Eq. 6 both support the view that rod responses are completely suppressed by the background. Second, the time to peak of the dim flash response was typically 70 ms, more than twofold briefer than the time to peak of any reported (even light adapted) mammalian rod response (Fig. 2, A and D; Table I). Third, the so-called dominant recovery time constant ("Pepperberg" constant), estimated from responses in the "just saturating" flash intensity regime, was typically ~70 ms, almost threefold shorter than that (~200 ms) typically reported for WT rods (Fig. 2, C and F; Table I). Fourth, the absolute sensitivity of the light responses to 361-nm flashes from WT retinal slices recorded in the presence of the background is comparable to that for the cells recorded in the absence of the background for cells from retinal slices of $G_t\alpha^{-/-}$ mice, and >40-fold lower than that of rods (Table I). Rods of $G_t\alpha^{-/-}$ mice are structurally normal, but do not respond electrically to light (Calvert et al., 2000). (The effect of the background on the cone responses is considered further below.) Fifth, other properties of the responses obtained from retinal slices of $G_t\alpha^{-/-}$ mice (Fig. 2, G–L; Table I), including the amplification constant and dominant recovery time constant, are very similar to those of responses obtained from slices of WT retina in the presence of the background. Sixth, the spectral sensitivity of the responses was typically maximal at ~360 nm, the λ_{max} of mouse cone S-opsin (Fig. 3 A). (An exception is that responses recorded from slices taken from the most dorsal retina were maximally sensitive at ~510 nm, the λ_{max} of mouse cone M-opsin, as described below). We conclude that the responses obtained from WT retinal slices in the presence of the standard background indeed arise from cones and proceed to their further characterization.

Magnitude of the WT Cone Circulating Current

The saturating amplitude r_{max} of the photocurrent recorded from WT cones by drawing the perinuclear region into the suction pipette ranged up to 15 pA; for 7 of 29 WT cones, r_{max} was at least 9 pA (compare Table I). (A practical lower limit of ~4 pA was set by the need for adequate dynamic range to measure a dim-flash response, with peak amplitude of ≤20% of r_{max}.) Because the spatial distribution of the "inner segment" limb of the circulating current and the total area of the cone membrane drawn into the pipette are unknown, the only rigorous conclusion that can be drawn is that the total circulating current of a WT mouse cone must be at least 7 pA. However, the total cone circulating current is likely to be at least 15 pA (the largest recorded value), and could be considerably greater. Comparison of the measured r_{max} of WT cones with that obtained from

TABLE I

Physiological Properties of WT, $G_t\alpha^{-/-}$ and $Nrl^{-/-}$ Cones, and WT Rods of the Mouse

Genotype, cell type	V_{OS}	a_C	R_{max}	$\tilde{S}_F$	A	t_{peak}	τ_D	$I_{1/2}$	$I'_{1/2}$
(no. of cells)	μm^3	μm^2	pA	$\Delta R\%/(h\nu\ \mu m^{-2})$	s^{-2}	ms	ms	photons $\mu m^{-2}s^{-1}$	photons $\mu m^{-2}s^{-1}$
WT S-cone (n = 21)	14	0.2	6 ± 1	0.022 ± 0.004	4.5 ± 1.0	73 ± 5	73 ± 10	(1.8 ± 0.6) × 10^5	(1.2 ± 0.4) × 10^5
WT M-cone (n = 8)	14	0.2	8 ± 2	0.014 ± 0.002	3.2 ± 0.7	63 ± 5	68 ± 18	(2.5 ± 0.9) × 10^5	(1.3 ± 0.6) × 10^5
$G_t\alpha^{-/-}$ S-cone (n = 5)	14	0.2	7 ± 3	0.040 ± 0.020	2.7 ± 1.1	92 ± 7	113 ± 17	1.0 × 10^5	0.7 × 10^5
$G_t\alpha^{-/-}$ M-cone (n = 5)	14	0.2	4 ± 1	0.044 ± 0.012	2.1 ± 1.1	100 ± 14	114 ± 29	(0.4 ± 0.1) × 10^5	(0.3 ± 0.1) × 10^5
$Nrl^{-/-}$ S-cone (n = 8)	8.3	0.11	13 ± 5	0.048 ± 0.018	3.5 ± 1.4	91 ± 6	110 ± 4	–	–
WT rods (n = 26)	37	0.5	20 ± 6	2.7 ± 0.55	8.3 ± 1.4	205 ± 10	235 ± 20	350	–

Columns 2–10 present parameters of the cells whose type is identified in the first column: V_{OS} is the envelope volume of the outer segment, a_C the light collecting area (MATERIALS AND METHODS), R_{max} the saturating amplitude of the light response, $\tilde{S}_F$ the sensitivity of the normalized dim flash response, specified as percent of the saturating response per (photon μm^{-2}), A the amplification constant (Pugh and Lamb, 1993), t_{peak} the time to peak of the dim-flash response, and τ_D the dominant recovery time constant (cf. Fig. 2). $I_{1/2}$ is the half-saturating step intensity, uncorrected for pigment depletion, and $I'_{1/2}$ the value obtained when intensity is adjusted for pigment depletion (Fig. 6). Error terms are ±2 SEM.; the number of cells of each type is given with the genotype specification. Outer segment volumes were derived from electron microscopy, as reported in (Carter-Dawson and LaVail, 1979; Daniele et al., 2005). Sensitivity of S-cones was measured with 361 nm, and for M-cones and rods with 501-nm flashes. The flash sensitivity can be converted into units of percent circulating current suppressed per photoisomerization by dividing the value of $\tilde{S}_F$ by the cone collecting area, 0.2 μm^2 (i.e., by multiplying $\tilde{S}_F$ by 5). As such conversion was deemed inappropriate for WT M-cones and WT S-cones that coexpressed substantial fractions of M-opsin due to the light-adapting effect of the rod-suppressing 500-nm background (Fig. 5), flash sensitivities for all photoreceptor types were expressed in the same physical units. The time to peak has not be adjusted for the delay caused by the analogue filtering of the recording with the 8-pole, 20-Hz bandwidth filter used; measurements show this delay to be ~25 ms, which can be subtracted from all the tabulated values of t_{peak}. The number of cones used for the determinations of the half-saturating step intensities ($I_{1/2}$, $I'_{1/2}$) was smaller than the number of cones used for estimating the other parameters in a given row: the n's were 8 (WT S-cones), 6 (WT M-cones), 2 ($G_t\alpha^{-/-}$ S-cones), and 3 ($G_t\alpha^{-/-}$ M-cones); the two $G_t\alpha^{-/-}$ S-cones had nearly identical step sensitivities and so there is no error term.

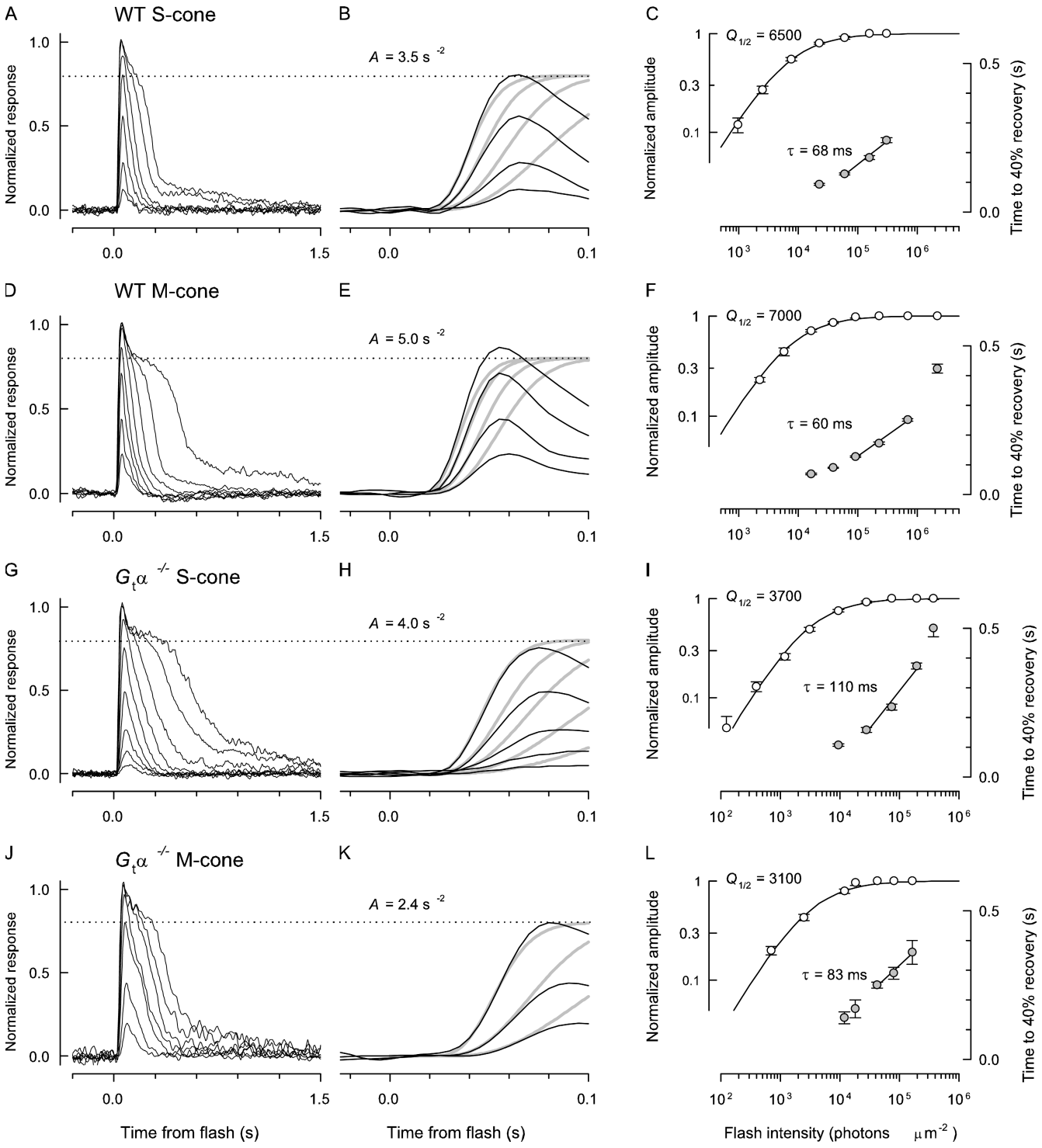

Figure 2. Kinetics and amplification of WT and $G_t\alpha^{-/-}$ mouse cone photoreceptors. Each row of three panels presents results obtained from a single mouse cone. The first column of panels presents families of light responses to a series of 20 μs (A, D, G) or 7 ms (J) flashes of graduated intensity. The second column of figure (B, E, H, and K) replots three to five of the traces in the first column on an expanded time base, but with the same vertical scaling; in these panels the amplification constant, *A*, of the responses is extracted by fitting the "LP" model of phototransduction (MATERIALS AND METHODS, Eq. 4) (thickened gray traces) to the rising phase of the responses (thinner black traces). As all cone responses exhibited a "nose" current (which decays rapidly after the peak of the responses to the most intense flashes), for the LP analysis the data were renormalized at the level of the dotted line, corresponding to 80% of the full response amplitude. The analyses in the third column of panels (C, F, I, and L) extract two additional kinetic parameters characterizing the response families: the half-saturating flash intensity $Q_{1/2}$ (photons μm^{-2}), obtained by fitting a hyperbolic saturation function (Eq. 5) to the response amplitude vs. intensity data (open circles, left ordinate)and the dominant recovery time constant, τ_D (ms), obtained from a "Pepperberg" analysis applied to the recovery times of the first three saturating responses (spanning ~1 $\log_{10}$ unit of intensity) of each

cones of the $Nrl^{-/-}$ mouse (Table I), whose outer segments are ~40% shorter, suggests that drawing several rod nuclei in the pipette may act to lower the current recording efficiency.

The Amplification of WT Mouse Cone Photoresponses

Amplification is a critical feature of the activation phase of the vertebrate photoreceptor light response (Lamb and Pugh, 1992; Pugh and Lamb, 1993), and the results show the responses of mouse cones to be highly amplified (Fig. 2, B, E, H, and K; Table I). Nonetheless, the analyses reveal that the cone amplification constants are two- to fourfold lower than that of rods recorded under the same conditions, and that the amplification of M-cones is somewhat lower than that of S-cones.

S- and M-opsins Are Coexpressed and Functional in WT Mouse Cone Photoreceptors

Histochemical evidence has revealed that most cones of C57Bl/6 ("WT") mice coexpress both S- and M-opsins, with the M-opsin expression varying in a dorso-ventral gradient (Applebury et al., 2000), and ERG b-wave evidence consistent with this conclusion has been published (Lyubarsky et al., 1999). Recently, we established such coexpression to occur in the all-cone retina of the $Nrl^{-/-}$ mouse and established with single-cell recordings that the coexpressed opsins are both functional, i.e., both capable of activating phototransduction in the same cone (Nikonov et al., 2005). In the current investigation, we confirmed these basic features in our recordings from single cones of the WT mouse but found a quantitative difference in the degree of expression of the M-cone opsin by the $Nrl^{-/-}$ and WT retinas.

Most WT mouse cones were found to be maximally sensitive at 360 nm, indicating that the majority of their opsin is S-cone opsin (Fig. 3 A). Nonetheless, 19/20 such cells exhibited a secondary mode of sensitivity at 510 nm, establishing that they functionally coexpress M-cone opsin. Such coexpression was found even in cones in slices of the most ventral portion of the retina, with one exception (Fig. 3, purple symbol identified by arrow). By recording from slices from the most dorsal part of the retina (MATERIALS AND METHODS), we found a subset of cones in which M-opsin was expressed to a higher degree than S-opsin (Fig. 3 A). By routinely measuring the sensitivity of all cones at both 361 and 501 nm, we obtained for each cone a spectral sensitivity ratio, S_{501}/S_{361}; cones for which this ratio exceeds unity will be classified as "M-cones," while those for which the ratio is less than unity will be designated "S-cones." The classification ratio varied systematically with the dorso-ventral position (Fig. 3). Because of the so-called β-band of absorption, which is maximal in the near UV for opsins with λ_{max} near 500 nm, and whose absorbance is ~20% that of the primary α-band (Govardovskii et al., 2000), it was not readily determinable whether all M-cones coexpress S-opsin. Thus, a few of the M-cones for which S_{501}/S_{361} was >5 could be pure "M-opsin cones."

Phototransduction Activated by the S- and M-cone Opsins in Individual WT Cones Is Very Similar

As both S- and M-cone opsins are expressed in individual WT cones and activate phototransduction in the same cell, it is of interest to ascertain whether the kinetics of the light responses driven by the two cone opsins are the same. Because of the wide separation in the λ_{max}'s of the two cone opsins, it is possible to unequivocally stimulate either the S- or the M-pigment in the S-cones (Fig. 3 A). While it was not possible, due to the problem of the absorption β-band (mentioned above), to unequivocally stimulate either opsin in all M-cones, in many cases it was. The results provide an unequivocal answer: in individual WT cones, the dim-flash responses driven by S- and M-cone opsins are effectively indistinguishable (Fig. 4).

Interestingly, the "dim-flash" responses of WT M-cones (t_{peak} = 63 ± 5 ms) are reliably faster than WT S-cones (t_{peak} = 73 ± 5 ms), and both are reliably faster than $G_t\alpha^{-/-}$ cones (t_{peak} = 90–100 ms) (Table I). (It bears mention that the 8-pole analogue filter used in the experiments produces a measured delay of ~25 ms, and the values of t_{peak} in Table I have not been corrected for this delay.) The question arises, however, whether these differences are intrinsic to the cone types or whether they may arise as a consequence of the use of a rod-suppressing background.

Most WT Cones Are Adapted by the Rod-suppressing Background due to M-opsin (Co)expression

We examined the hypothesis that the standard rod-suppressing 500-nm background, combined with the degree of expression of M-opsin in a given WT cone, might underlie the differences in dim-flash kinetics. Two qualitative predictions of the hypothesis can be readily

response family (filled circles, right ordinate). The data in the first two rows of panels (A, B, C; D, E, F) were obtained from retinal slices of WT mice in the presence of a rod-saturating background, while those in the third and fourth rows (G, H, I; J, K, L) were obtained from slices of $G_t\alpha^{-/-}$ in the absence of the background. The data in the first and third rows were obtained from cones maximally sensitive at ~360 nm ("S-cones") and were recorded in response to 361-nm flashes, while those in the second and fourth rows were from cones maximally sensitive at ~510 nm ("M-cones") and were recorded in response to 501-nm flashes. All responses were filtered during acquisition with an 8-pole low pass analogue filter set at 20 Hz and digitized at 200 Hz. At least 15 responses to the same flash intensity were averaged for each trace, and at least 30 for responses to the dimmest flashes. The saturating response amplitudes were 6 pA (A), 15 pA (D), 11 pA (G), and 4 pA (J).

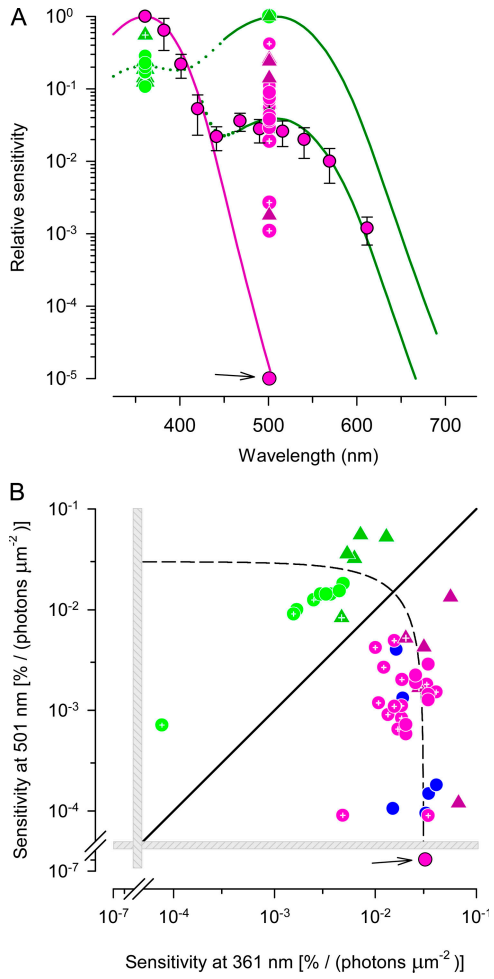

Figure 3. Spectral properties of WT and $G_t\alpha^{-/-}$ mouse cone photoreceptors. (A) Spectral sensitivities. Data of all cones have been normalized at either 361 or 501 nm, depending on the wavelength of maximal sensitivity. Purple filled circles with error bars plot sensitivity results of a single WT cone: the data are fitted with the sum of two pigment templates (Lamb, 1995), the mouse cone S-opsin (λ_{max} = 360 nm, smooth purple curve) and the mouse cone M-opsin (λ_{max} = 508 nm), with the latter scaled by 0.039 (lower smooth green curve). The upper green curve is the same template, normalized; the dotted portion of the curve is a possible extension of the template (Govardovskii et al., 2000). For other cones, results from only 361 and 501 nm are plotted. Data of WT mice are plotted as circles, and data from $G_t\alpha^{-/-}$ mice as triangles. Data from cones in retinal slices dissected from the most ventral portion of the retina (see MATERIALS AND METHODS) were invariably maximally sensitive at 361 nm and are plotted as purple filled circles, while data from cones in retinal slices from the most dorsal portion of the retina were invariably more sensitive at 501 nm and are plotted as green filled circles. Data obtained from cones in retinal slices of unknown location are colored according to the wavelength of maximal sensitivity 361 (purple) or 501 nm (green), but are shown with embedded white cross-hairs. One cone maximally sensitive at 361 nm had a sensitivity at 501 nm that matched the template (arrow), and thus is inferred to express only S-opsin. (B) Classification of WT, $G_t\alpha^{-/-}$, and $Nrl^{-/-}$ cones according to their relative sensitivities at 361 and 501 nm. Each point plots the absolute sensitivity of one cone at 501 nm (ordinate) vs.its absolute sensitivity at 361 nm, with sensitivity expressed in percentage of circulating current suppressed per photon μm^{-2}. The same symbol scheme is used as in A; data from $Nrl^{-/-}$ cones recorded in the "OS-out" configuration (Nikonov et al., 2005) are plotted as filled blue circles. The diagonal (unity slope line) plots the locus of cones that would be equally sensitive to 361- and 501-nm light; cones that plot above this line are considered "M-cones" and those lying below it "S-cones." The dashed line plots a locus defined by $S_{361} + S_{501} = 0.03$, which would describe the data if total cone opsin expression were conserved and both opsins drove phototransduction with equal efficiency. The data of the one "pure S-cone" is again identified by an arrow. (The gray hatched bars have been added to emphasize the nearly 2 $\log_{10}$ unit break in the axes.)

made: (1) t_{peak} should be a decreasing function of the degree of M-opsin coexpression by S-cones, and (2) flash sensitivity should be a decreasing function of the degree of M-ospin coexpression. Two additional predictions can be made on the hypothesis that the properties and recordings of $G_t\alpha^{-/-}$ cones differ from those of WT only in that no background was needed to isolate their responses: (3) t_{peak} of the cones of $G_t\alpha^{-/-}$ mice should not depend on the degree of expression of M-opsin, and (4) t_{peak} of WT S-cones should approach t_{peak} of $G_t\alpha^{-/-}$ S-cones for low M-opsin coexpression. These predictions are reasonably well confirmed (Fig. 5 A).

The prediction (2) (Fig. 5 B) that sensitivity should decline with the degree of M-opsin coexpression can be made quantitative by using the general hypothesis (a) that mouse cones obey Weber's Law, and assuming in addition (b) that the total opsin content of the mouse cone is fixed (i.e., S-opsin + M-opsin = const), and (c) that (except for their spectral sensitivities) the two cone opsins are identical in their properties. The latter properties include in particular the rate at which fully active S- and M-opsin activate cone transducin (Gnat2), and the time course with which they are inactivated by Grk1. Given the spectra of the two cone opsins and these assumptions, the ratio ρ of expression of M-opsin to S-opsin (the "M-opsin co-expression ratio") corresponds closely to the sensitivity ratio, i.e., $\rho = S_{501}/S_{361}$. Using the conservation assumption (b), one finds the fraction of M-opsin in a cone satisfies $f_{MOps} = \rho/(\rho + 1)$, while the fraction of S-opsin is $f_{SOps} = 1 - f_{MOps}$. And so one arrives at the quantitative relations

$$S_F(I_{500}, \rho, \lambda) = \frac{S_{F,dark}(\lambda) f_{MOps}}{1 + \left[\frac{I_{500} a_C f_{MOps}}{I_{dark}^*}\right]}, \quad \text{for } \lambda = 501 \text{ nm} \tag{7A}$$

and

$$S_F(I_{500}, \rho, \lambda) = \frac{S_{F,dark}(\lambda) f_{SOps}}{1 + \left[\frac{I_{500} a_C f_{MOps}}{I_{dark}^*}\right]}, \quad \text{for } \lambda = 361 \text{ nm}, \tag{7B}$$

where S_F is the sensitivity of a cone with coexpression ratio ρ measured with a flash of wavelength λ (=501 or 361 nm) in the presence of the standard background of intensity I_{500} (=20,000 photons μm^{-2}), a_C = 0.2 μm^2 is the collecting area of a cone expressing only one opsin, I_{dark}* is the "dark light" expressed in an equivalent isomerization rate, and $S_{F,dark}$ is the dark-adapted sensitivity of such a cone in the absence of the background. The theoretical curve generated by Eq. 7 is plotted as the dark gray line in Fig. 5 B; for ρ < 1, it exhibits a familiar Weber Law dependence on ρ. Again using hypothesis (c) that cones of $G_t\alpha^{-/-}$ mice differ only from those of WT in that no background was needed to isolate them, one predicts that the sensitivity of WT S-cones that coexpress low levels of M-opsin should asymptote (ρ→0) to the sensitivity of $G_t\alpha^{-/-}$ cones; this is indeed observed. In addition, as expected, all the WT M-cone sensitivities, unlike some of the WT S-cone sensitivities, lie reliably below those of the $G_t\alpha^{-/-}$ mice. The principal discrepancy between prediction and observations is that the sensitivities of the WT M-cones lie systematically above the theory line (Fig. 5 B, green symbols). Possible reasons for the discrepancy include a violation of one or more of the assumptions (a –c) underlying the derivation. Future physiological experiments will address the issue of whether the cones obey Weber's Law, and whether the S- and M-opsins are inactivated with the same kinetics by Grk1. Biochemical experiments will be required to assess potential differences in the S- and M-opsins in activating Gnat2.

In summary, then, we conclude that the degree of coexpression of M-opsin in WT mouse cones leads to varying degrees of desensitization and speeding of the dim-flash response kinetics (shortening of t_{peak}) by the rod-suppressing background, and conclude further that the results are generally consistent with the notion that

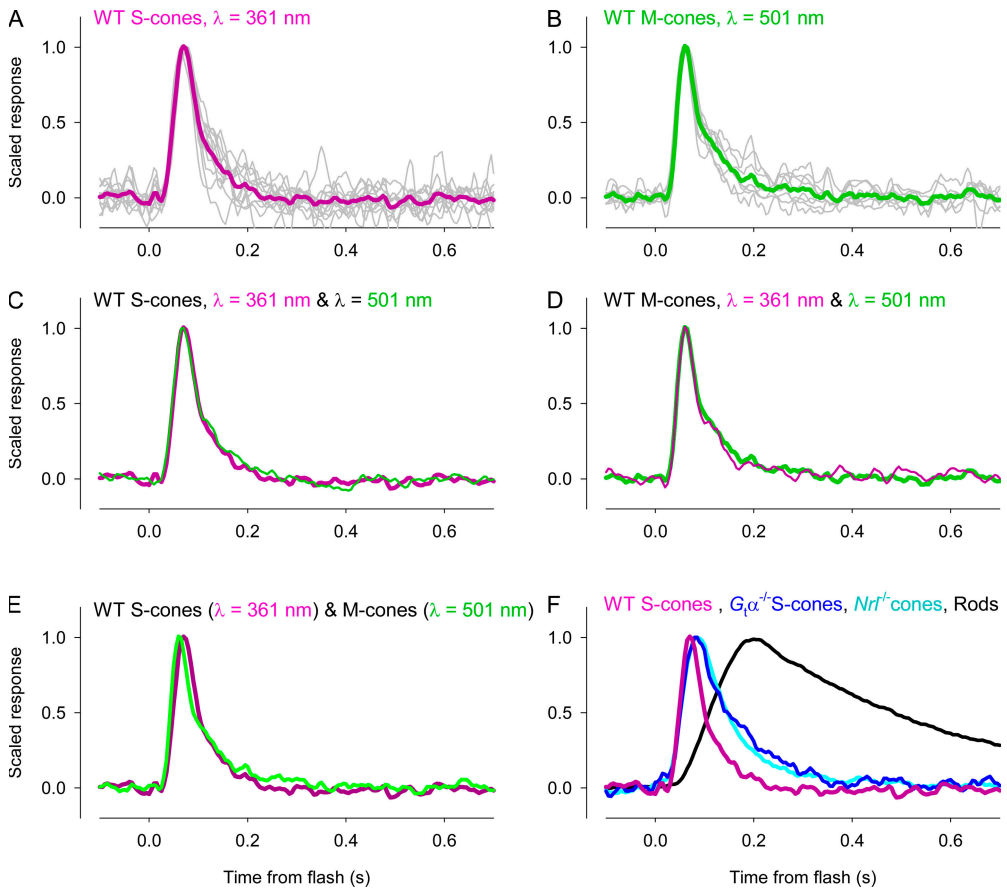

Figure 4. Dim-flash responses of cone photoreceptors of WT and $G_t\alpha^{-/-}$ mice. Cones were classified as S-cones or M-cones according to Fig. 3 B. (A) Dim-flash responses to 361-nm flashes of individual S-cones (gray noisy traces) and their average (purple trace). (B) Dim-flash responses of individual M-cones to 510-nm flashes (gray traces) and their average (green trace). (C) Average dim-flash response of S-cones to 361-nm flashes (purple trace, repeated from A) and to 510-nm flashes (thinner, green trace). (D) Average dim-flash response of M-cones to 510-nm flashes (green trace, repeated from B) and to 361-nm flashes (thinner, purple trace). (E) Comparison of the average response of S-cones to 361-nm flashes (purple trace) and M-cones to 510-nm flashes (green trace). (F) Comparison of the grand average dim-flash responses to 361-nm flashes of WT S-cones (purple trace), $G_t\alpha^{-/-}$ S-cones (blue), $Nrl^{-/-}$ cones (cyan, n = 7, recorded in the "OS-out" configuration), and 26 rods (gray trace) recorded under the same conditions (Nikonov et al., 2005). Each trace is scaled to unity at its peak.

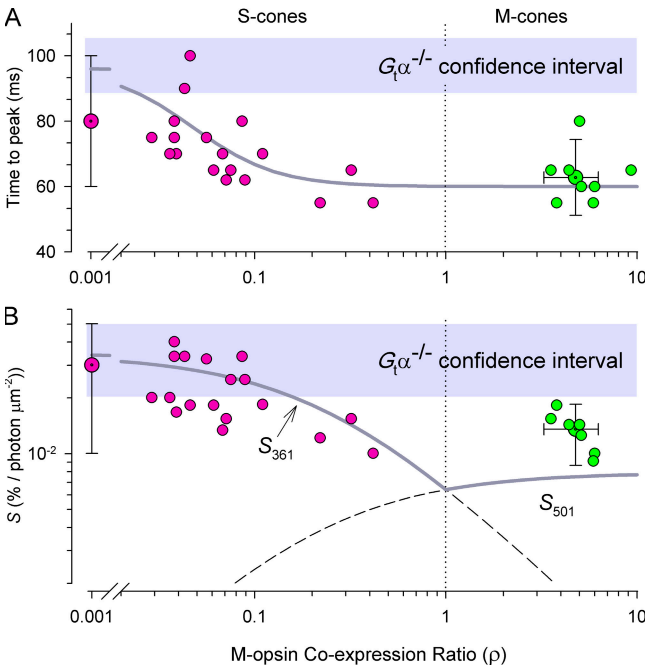

Figure 5. Effect of M-opsin expression level on kinetic features of the dim-flash response. (A) Time to peak of the dim-flash response (c.f., Fig. 4, Table I) plotted as a function of the estimated M-opsin coexpression ratio. (B) Flash sensitivity (% saturating response per photon μm^{-2}). The M-opsin coexpression ratio ρ was estimated as the relative sensitivity to 501- and 361-nm flashes, i.e., for each cone $\rho = S_{501}/S_{361}$ (compare Fig. 3) was measured. Each point plotted without error bars represents data of a single cone: for S-cones (red filled circles) $\rho < 1$; for M-cones (green filled circles) $\rho > 1$; error bars are 95% confidence intervals for pooled data (data for several S-cones with $\rho \leq 0.001$ were pooled and plotted at $\rho \approx 0.001$; the points in the M-cone sector with bidirectional error bars provide the mean and 95% confidence intervals for the entire M-cone populations). The gray bars plot 95% confidence region for the time to peak (t_{peak}) and dim-flash sensitivity of $G_t\alpha^{-/-}$ cones; since there were no trends in these cones, their results were pooled (see Table I). The smooth (gray) curve in A plots an empirical relation, $t_{peak}(\rho) = t_{peak,dark} - \Delta t_{peak}[\rho^n/(\rho^n + \rho_0^n)]$, with $t_{peak,dark} = 96$ ms, $\Delta t_{peak} = 36$ ms, $n = 2$, $\rho_0 = 0.048$; 96 ms is the overall mean t_{peak} for $G_t\alpha^{-/-}$ cones, while Δt_{peak} was selected so the curve would run through t_{peak} for the M-cones. The gray curve in B plots the upper envelope of Eqs. 7a and 7b; the extension of the individual curves for S_{361} and S_{501} are shown as dashed lines. Eq. 7 has two parameters $S_{F,dark}$ and I_{dark}*; we set $S_{F,dark} = 0.034$, close to the average value for $G_t\alpha^{-/-}$ cones (Table I), and $I_{dark}* = 1200\ s^{-1}$.

the properties of fully dark-adapted WT cones can be inferred from those of $G_t\alpha^{-/-}$ cones, whose isolation does not require the use of backgrounds.

Step Responses of S- and M-cones

Cones differ from rods in their responsivity to steady light (INTRODUCTION), and so we undertook experiments to determine how mouse cones responded to light steps of varied intensity (Fig. 6). Both S- and M-cones reached steady state in ~100 ms and recovered their full circulating current from even the most intense steps used in ~1 s when the step was extinguished (The recovery from the steps was determined in experiments with $G_t\alpha^{-/-}$ retina, in which there was no rod current suppression [Fig. 6, E and G].) The step response vs. intensity relations were characterized with hyperbolic saturation relations (Eq. 6); population averages of the half-saturating intensities are provided in Table I. Taken at face value, the data suggest that the cones of $G_t\alpha^{-/-}$ retinas were more sensitive to light steps, a surprising result given that the cones of $G_t\alpha^{-/-}$ mice appear to have somewhat lower amplification. One possible explanation for the discrepancy is that the sensitivity of the WT cones was lowered by bleaching by the rod-suppressing backgrounds, in effect lowering their collecting area. We suspected that substantial fractions of the M-cone pigment were bleached during the course of the step experiments, as the rod currents in records from WT retinal slices were persistently suppressed. We thus developed a rigorous approach to calculating the level of bleached pigment at any time in the experiment, applying Eq. 3 to the sequence of stimulations. These analyses confirm that at least part of the discrepancy in step responsivity between $G_t\alpha^{-/-}$ and WT cones was due to cone pigment bleaching; thus, the corrected data and saturation curves (Fig. 6, gray symbols and traces) bring the WT cone results into closer agreement in regards with those of $G_t\alpha^{-/-}$ cones, reducing the estimates of $I_{1/2}$ in WT cones by two- to threefold. Even with a blanket threefold adjustment for bleaching, however, the WT cones appear to be less sensitive to steps than $G_t\alpha^{-/-}$ cones, suggesting that WT cones may possess some capacity for light adaptation that is attenuated in the $G_t\alpha^{-/-}$ retina.

Bleached M- and S-opsin Activate Phototransduction to Differing Degrees in Mouse Cones

Estimation of the amount of pigment bleached during experimentation with mouse cones led us to examine the manner in which bleached pigment activates phototransduction in these cones, leading to suppression of the circulating current and to compare this suppression with that in rods in which various amounts of rhodopsin were bleached (Fig. 7 A). The bulk of the bleaching of the cone pigments was done in several minutes, although some bleaching had occurred earlier in the experiment during the time course of the stimulation used to obtain flash response families (~30 min total). Cone circulating current was invariably found to reach steady state at the termination of the bleaching exposure within the few seconds needed to make a reliable measurement. In contrast, for rods it was necessary to wait many minutes after bleaching for achievement of a steady-state recovery of the circulating current; ~15 min were required for the lower bleaching levels and up to 30 min for the largest bleaching exposures. For both rods and cones, once reached, the steady state was

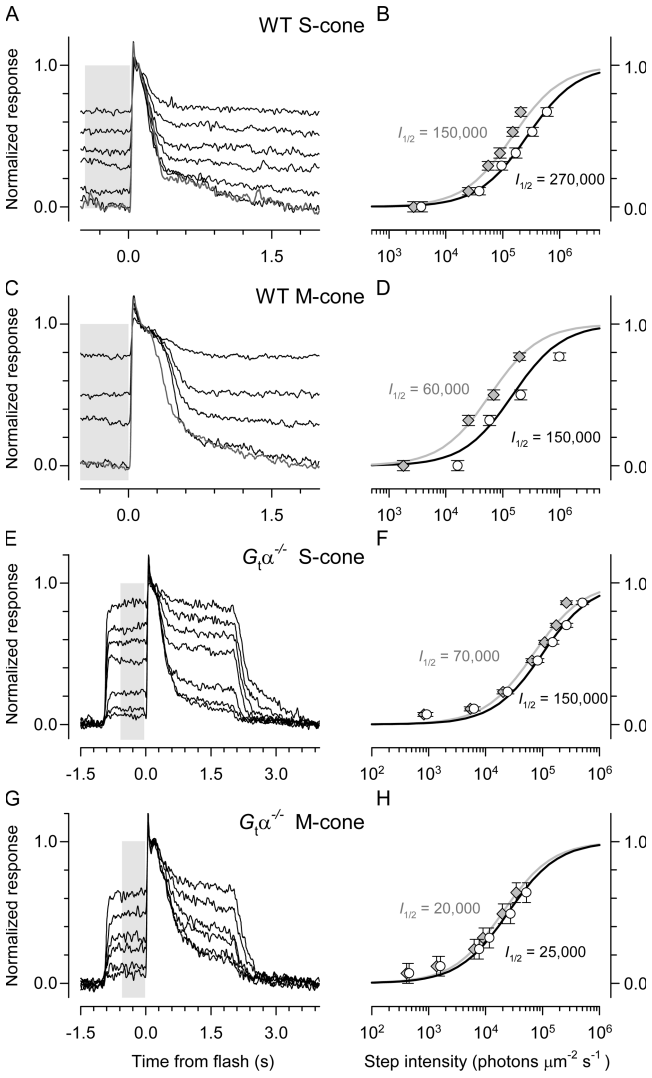

Figure 6. Responses of WT and $G_t\alpha^{-/-}$ mouse cone photoreceptors to steps of light of graded intensity. A, C, E, and G present the responses of cones of mice of the genotype indicated on the figure to steps of light, while B, D, F, and H present the response amplitude vs. step intensity relation for the same cone. Thus, each point plotted in the righthand panels corresponds to the average amplitude of the step response in the portion of the plot at left illustrated on a gray background. For the S-cones (A, B; E, F), steps of 361-nm light were used; for the M-cones (C, D; G, H), steps of 501-nm light. The timing of the delivery steps and flashes in experiments with WT cones is illustrated in Fig. 1 D; in these experiments, the steps also suppressed rod activity, but as the initial re sponse to the step need not reflect cone activity alone, it is omitted. In the experiments with $G_t\alpha^{-/-}$ retinas there was no rod activity, and so the initial response to the step reflects the time course of the cone response (note the different time scales in A, C vs. E, F). To accurately determine the fractional response (i.e., the fraction of the cone's circulating current suppressed by the background), a very strong flash was delivered in each cycle of presentation of the steps: the data in A, C, E, and G are aligned with respect to this flash ($t = 0$). The response vs. intensity data were fitted with a hyperbolic saturation relation (Eq. 6); the fitted curve (black smooth trace) and the estimated intensity $I_{1/2}$ of the step that produces a response of half-maximal amplitude in each case are given on the panels to the right of the data. Each response illustrated corresponds to between 10 and 20 repetitions of the light step, and the traces are the average, normalized by the response to the saturating flash presented in the presence of the dimmest step (the standard background) (A and C) or presented in darkness (E and G). For the WT cones, the averaged response to the saturating flash in the presence of the standard background after the series of step presentations is shown as the cyan trace. The gray symbols replot the response amplitude data on an intensity axis adjusted for the decrease in collecting area due to the depletion (bleaching) of the cone pigment by light stimuli presented before the steps were delivered, calculated by applying Eq. 3 to the data. The hyperbolic saturation relations fitted to these "bleach-corrected" data are shown as the smooth gray traces, with $I_{1/2}$ given to the left of the data and smooth curve.

maintained for 10 min or more (at which time the experiments were usually terminated).

The relationship between bleached opsin and steady-state circulating current appears to be quite different for the three mouse opsins, with bleached rhodopsin being far more active than the two cone opsins, but bleached S-opsin considerably more active than bleached M-opsin, which appears to have almost no effect (Fig. 7 B). Remarkably, several M-cones with >90% of their M-opsin bleached had circulating currents almost equal to the dark-adapted level. It is worth emphasizing that the calculations with Eq. 3 of the fraction of rhodopsin bleached in a rod and M-opsin bleached in an M-cone by the same light stimuli are almost identical, because of the close proximity of the λ_{max}'s of these two pigments.

DISCUSSION

Cone Vision Is Robust in Mice and Responses from Single Cones Can Be Recorded

Cones provide the signals for the daytime vision of all mammals. Although mice are often characterized as nocturnal and "rod dominant," cone signaling is clearly of great importance to their survival. The ultraviolet sensitivity of mouse S-cones, which are more concentrated in the ventral retina, looks to the sky and likely enhances the ability of mice to detect predatory raptors during daytime foraging excursions (Rowe, M.P. 1999. *Invest. Ophthalmol. Vis. Sci.* 40:3970). The importance of cone vision to mice is also clearly revealed by the density of cones and the commitment of post-receptor retinal circuitry to processing cone signals. Indeed, the mouse retina has a considerably higher cone density (~10,000 mm^{-2}) than the peripheral retina of primates (~3,000–5,000 mm^{-2}) (Carter- Dawson and LaVail, 1979; Jeon et al., 1998; Ghosh et al., 2004). Moreover, like primates, mice have 10 highly conserved types of bipolar cells, and 9 of these (constituting approximately one half the total bipolar cell population and including four OFF-bipolars and five ON-bipolars) make exclusive contact with cones (Ghosh et al., 2004). The robust mouse

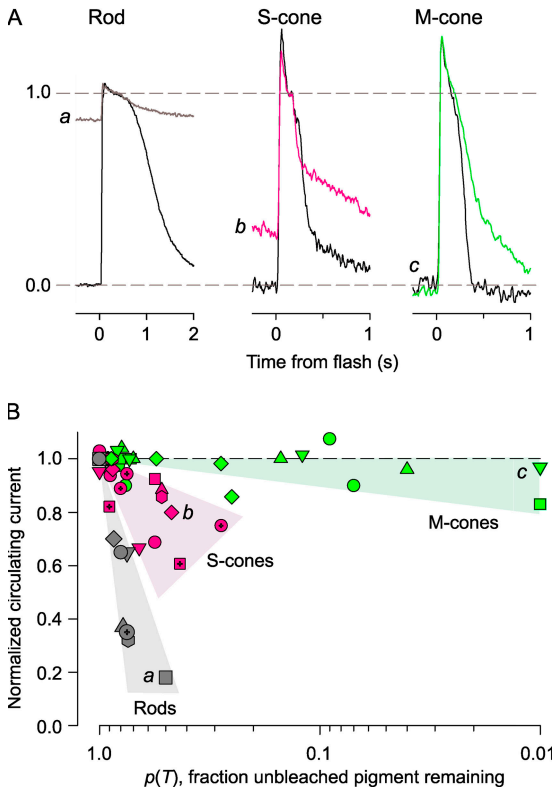

Figure 7. Bleached S- and M-cone opsins and rhodopsin persistently activate phototransduction to different degrees. (A) Saturating responses of a rod, S-cone, and M-cone before (black trace) and after (colored traces; a, b, c) light exposures that bleached substantial fractions of their respective visual pigment. The fractions of the pigments bleached at the time of the second response were calculated with Eq. 3, and were 60% (rhodopsin in rod), 53% (S-opsin in S-cone), and 99% (M-opsin in M-cone). (B) Normalized circulating current as a function of the fraction p(T) (Eq. 3) of the total opsin in the unbleached state at the time T when a saturating flash was delivered to WT S-cones (purple symbols), M-cones (green symbols), and rods (gray symbols). The absolute amplitudes of the initial responses (black traces) in the top panels were 40 pA (Rod), 5.0 pA (S-cone), and 12.5 pA (M-cones). (The rod response likely arose from two nuclei in the suction pipette, as confirmed single rods were rarely found to yield >25 pA.) The smaller amplitude traces in the top panels are labeled with letters, a, b, c; these letters have been placed next to the points in B to which they correspond.

cone-driven ERG b-wave, whose amplitude is approximately one third of the total rod- and cone-driven b-wave of a dark adapted mouse, is consistent with the histological evidence (Lyubarsky et al., 1999). The b-wave is generally held to be the field potential arising from light-dependent inactivation of mGluR6 metabotropic receptors in the dendritic terminals of ON-bipolar cells (Robson et al., 2004). Nonetheless for the importance of cone signaling in the mouse retina, perhaps because of the 30-fold higher numerosity of rods, or because of the fragility of cone outer segments separated from their extracellular matrix sheaths (Nikonov et al., 2005), mouse cones have been an elusive target for electrophysiological characterization at the single-cell level.

Using a retinal slice preparation and a novel method of recording in which several outer nuclear layer nuclei and adjacent tissue is drawn into a suction pipette (Fig. 1), we have now recorded and characterized for the first time the electrical responses of single WT mouse cones. At least six distinct lines of evidence and arguments support this contention: the overall thrust is that the photoresponses recorded in the presence of a 500-nm background of ~20,000 photons $\mu m^{-2}s^{-1}$ have properties that are (a) highly distinct from the corresponding properties of mouse rods, (b) specifically predicted for mouse cones (e.g., peak sensitivity in the near UV), or (c) generally expected of mammalian cones, but not rods.

S-cones, M-cones, and Functional Coexpression of S- and M-cone Pigments in WT Mouse Cones

Mouse cones can be classified as "S-cones" and "M-cones" based on which of the two mouse cone opsins drives phototransduction with a higher sensitivity (Fig. 3 B). Our experiments, as expected from previous immunohistochemical (Rohlich et al., 1994; Applebury et al., 2000; Lukats et al., 2002) and electroretinographic (Calderone and Jacobs, 1995; Jacobs et al., 1991; Lyubarsky et al., 1999) investigations, establish that most WT mouse cones are maximally sensitive at 360 nm, and thus are classified as S-cones. Our experiments also show that WT, unlike *Nrl*$^{-/-}$ mice (Nikonov et al., 2005), have M-cones in their dorsal retina (Fig. 3 B), as expected from immunohistochemistry (Applebury et al., 2000). While the physiological evidence is still incomplete, we nonetheless suspect that a very high percentage of mouse cones coexpress both S- and the M-cone opsins, in part based on previous electroretinographic results (Lyubarsky et al., 1999). Nearly universal coexpression of M-opsin is clear for the S-cones, for which the action spectrum analysis can detect M-opsin coexpression to as low as 1 part in 10,000 (Fig. 3 A): only one S-cone in >30 recorded to date follows the template for a 360-nm opsin at 500 nm (Fig. 3). For M-cones, universal coexpression of S-opsin is not certain, as the β-band of the M-opsin prohibits detection in dark-adapted cones of S-opsin coexpressed at a ratio less than approximately one fourth (Fig. 3). Future experiments in which systematic bleaching of M-opsin is employed should allow definitive determination of the sensitivity of the M-opsin β-band, and detection of S-opsin in "M-cones" coexpressed <1%.

The likely nearly universal coexpression of the two cone opsins and the dorso-ventral gradient of M-opsin coexpression to some extent render a two-category classification of mouse cones moot and misleading, and it may be more useful in many contexts to speak of "S-dominant" and "M-dominant" cones. For example,

experimenters not equipped to stimulate the mouse retina with UV light might draw erroneous conclusions about the sensitivity and adaptational properties of cone-driven inner retinal neurons. Indeed, M-opsin coexpression may lead physiologists characterizing the light responses of cone-driven bipolars and other postreceptor cells in the mouse (e.g., Berntson and Taylor, 2000) to misestimate their true sensitivity, which would only be seen with UV stimulation

Physiological Features of WT Mouse Cones

Absolute Sensitivity. The effects of the coexpression of M-opsin and the requirement for a rod-suppressing background lead to an underestimation of the absolute sensitivity of both WT S- and M-cones, but all the data of WT and $G_t\alpha^{-/-}$ cones become mutually consistent when these effects are taken into consideration (Fig. 5); ~0.2% of the WT mouse cone circulating current is suppressed per photoisomerization at the peak of the dim-flash response. For rods recorded under the same condition, absolute sensitivity is ~5% (these values can be obtained from the sensitivities in Table I by converting the flash intensities into photoisomerizations by multiplying by the collecting areas, $a_C = 0.2\ \mu m^2$ [cones] and $a_C = 0.5\ \mu m^2$ [rods]). Closely comparable values have been reported for rods and cones of primates (Baylor et al., 1984; Schnapf et al., 1990).

Dim-flash Kinetics. Dim-flash responses driven by the two cone pigments in individual WT mouse cones are effectively indistinguishable, whether the cone is classified as an S-cone or M-cone (Fig. 4). This result provides support for the hypothesis that the phototransduction cascades activated by the S- and M-cone opsins are (other than the photopigments) identical. Support for this conclusion also comes from genomic evidence that there is only one additional G-protein α-subunit, Gnat2, that is highly homologous to rod transducin ($G_t\alpha$) (Wilkie et al., 1993), combined with histochemical evidence that this protein is universally expressed in vertebrate cones (Lerea et al., 1986, 1989; Ying et al., 1998).

Amplification. For the first time, we are able to compare the amplification of the S- and M-cone pigments: in both WT and $G_t\alpha^{-/-}$ M-cones, the amplification constant A appears to be reduced by 20–30% relative to that of S-cones (Table I). But as this apparent reduction is small, in the context of the very similar absolute sensitivities and dim-flash kinetics of the two cone types, it seems likely that fully active S- and M-cone opsins activate Gnat2 (cone transducin) at approximately the same rate. The amplification constants of the cones are, however, very reliably below that of rods, by a factor of two- to threefold (Table I). One of the factors (β_{sub}, the rate constant of a single phosphodiesterase (PDE) catalytic subunit in the outer segment) that multiply to produce the amplification constant is inversely proportional to the outer segment volume (Lamb and Pugh, 1992; Pugh and Lamb, 1993), and the cone outer segment volume is only 40% that of the rods (Table I). On the assumption that the catalytic efficiency k_{cat}/K_m of the cone PDE is the same as that of the rods (Gillespie and Beavo, 1988), it follows that PDE catalytic subunits in mouse cones are activated per fully active cone "R*" at a rate less than one fifth that at which rod PDE catalytic subunits are activated per fully active rhodopsin, R*. Alternatively, k_{cat}/K_m for mouse cone PDE may be lower than that of rod PDE, and if so, this would contribute to the lower overall amplification.

Opsin Inactivation. Grk1 is the only GPCR kinase in the mouse kinome that is expressed in mouse photoreceptors (Weiss et al., 2001; Chen et al., 2001; Caenepeel et al., 2004), and it is now clear that Grk1 is necessary for normal inactivation of both mouse cone opsins (Lyubarsky et al., 2000; Nikonov et al., 2005). Given the kinetics of the responses driven by S- and M-opsins (whether these occur in S- or M-dominant cones) (Fig. 4), it follows that Grk1 largely inactivates both cone opsins in well less than 50 ms, the inflection point in the activation phase of the dim-flash response, at which the response begins to "peel downward" from the pure activation theory. The almost twofold faster inactivation of mouse cone opsins than rhodopsin by the same kinase, Grk1, argues that this kinase is more effective in mouse cones than in mouse rods, either due to its specific affinity for the S- and M-opsin, or due to its level of expression.

Dominant Recovery Time Constant. Compelling evidence has recently been presented that the dominant recovery time constant of mouse rods arises from the time constant of the GTPase activity set by the interacting complex of the transducin α-subunit ($G_t\alpha$), the phosphodiesterase γ-subunit (PDEγ), and regulator of G-protein signaling, Rgs9-1, coupled to its anchor protein R9ap (Krispel, C.M., C.K. Chen, D. Chen, Y.J. Chen, N. Calero, and M.E. Burns. 2005. Invest. Ophthalmol. Vis. Sci. 46:4628). It is generally accepted that the dominant recovery time constant, τ_D, originates in the inactivation of one or the other of the two principal amplifiers of the phototransduction cascade, the photoactivated pigment R* (in which case, $\tau_D = \tau_R$) or the activated PDE complex, $G_t\alpha$-PDE (in which case, $\tau_D = \tau_E$) (compare Nikonov et al., 1998, 2000). From the observation that $\tau_D \approx 70$ ms in mouse cones (Fig. 2; Table I), it can be concluded that τ_E is considerably shorter in mouse cones than in mouse rods, likely sped up by a higher level of expression of RGS9-1 in cones as opposed to rods (Lyubarsky et al., 2001; Zhang et al., 2003). Our results, however, do not speak to the issue of which of the two cascade amplifier inactivation steps is dominant

in mouse cones, but only imply that both τ_R and τ_E are shorter than the slower step in mouse rods.

The "Nose" on the Photocurrent. The saturating photoresponses of WT and $G_t\alpha^{-/-}$ cones exhibit a "nose," a current that has the same sign as the photocurrent, and which undergoes a rapid decay to a plateau with a time constant <50 ms (Figs. 2 and 6). The photocurrent, recorded from the inner segment plasma membrane in the configuration employed in the experiments reported here, is largely due to a decline in a K^+ current (I_{Kx}) that tracks the light-activated decline of the cGMP-activated current of the outer segment (Frings et al., 1998). A likely explanation of the "nose" is that it is due to the inwardly rectified, hyperpolarization-activated current, I_h (Hestrin, 1987). Strong flashes that completely close the cGMP-activated channels should hyperpolarize the cone below the reversal potential of I_h and trigger a depolarizing current, as observed. (For simplicity in presentation, we have shown all light responses as positive-going deflections. However, in the "inner segment in" recording configuration used here, the responses are the suppression of an outward membrane current.) This same current is clearly present and of comparable magnitude in responses of $Nrl^{-/-}$ cones as in WT cones, but less prevalent in rods (Nikonov et al., 2005). A practical consequence of this current is that it makes it more difficult to define the saturating level of the photocurrent (Figs. 2 and 6), impacting on the precision of estimating various parameters characterizing the cells.

WT Mouse Cones Can Function "Normally" with Large Fractions of their Opsin Bleached

Differences amongst the three types of mouse opsin were revealed in the apparent degree to which bleached rhodopsin, S-opsin, and M-opsin causes persistent suppression of the circulating current (Fig. 7). A "dark light" generated by bleached rhodopsin has been well documented in recordings from amphibian (Lamb, 1981; Cornwall and Fain, 1994; Matthews et al., 1996), and primate (Baylor et al., 1984) rods, and also in salamander (Cornwall et al., 1995) and primate (Schnapf et al., 1990) cones. As revealed in recent experiments with the human cone ERG a-wave (Kenkre et al., 2005), however, mammalian cone transduction is vastly less activated by cone opsin dark light than is rod transduction by bleached, unregenerated rhodopsin. Our results suggest that different classes of cone opsin may differ in regards to their generation of dark light, with bleached S-opsin acting somewhat more like bleached rhodopsin, and bleached M-opsin having almost negligible effect, as expected from its close homology with human M- and L-cone pigments (Kenkre et al., 2005). The coexpression of the two opsins in mouse cones may prove useful in the investigation of these differences, and we are actively pursuing the problem.

WT, $G_t\alpha^{-/-}$, and $Nrl^{-/-}$ cones: Preparations for the Investigation of Mammalian Cone Function

In two recent reports, we presented a body of results, including electron microscopy, immunohistochemistry, quantification of key cone transduction proteins, ERG a-wave analysis, and single-cell recordings, that together establishes that the photoreceptors of mice lacking the neural leucine zipper transcription factor ($Nrl^{-/-}$) are cones (Daniele et al., 2005; Nikonov et al., 2005). The results presented here, which characterize the physiological features of WT mouse cones, show that $Nrl^{-/-}$ photoreceptors are in fact practically indistinguishable from WT cones in their physiological features (Table I). These results thus close that case on the identification of the $Nrl^{-/-}$ retina as an "all-cone" retina and further strengthen the case for its use in the investigation of cone-specific genes and their function. Nonetheless, several exceptional features call for caution.

The first exception is that $Nrl^{-/-}$ cone outer segments are on average only 60% the length of WT cone outer segments, and that they exhibit a degree of disorder of their disc stacking and overall orientation (Daniele et al., 2005). The second exception is that $Nrl^{-/-}$ cone outer segments undergo a slow degeneration that results in the halving of the circulating current by 6 wk of age (Daniele et al., 2005). The third exception is that $Nrl^{-/-}$ cones do not express M-cone opsin to the same degree as WT cones. This latter point is supported by the observations presented here (Fig. 3 B), and also by comparison of the action spectrum of the cone-driven b-wave of the WT mouse (Lyubarsky et al., 1999) with that of the a-wave of the $Nrl^{-/-}$ mouse (Daniele et al., 2005); the secondary mode (at 510 nm) of the action spectrum of the WT mouse cone system is approximately one fourth the sensitivity of the primary mode (at 360 nm), but in the $Nrl^{-/-}$ mouse, the secondary mode falls to one eighth or less. Nonetheless, for these exceptions, the definitive conclusion that photoreceptors in the $Nrl^{-/-}$ mouse in the first 6 wk of life are healthy cones opens the door to many investigations of importance to the understanding of function of genes expressed specifically in cones.

We are grateful to Peter Calvert, Lauren Daniele, Arkady Lyubarsky, and Trevor Lamb for helpful comments on this work. Also, we are very grateful to Tonia Rex for the confocal images used for the cover of this issue, and to Tom Hughes for providing mice expressing EGFP under the human L/M cone promoter.

This work was supported by NIH-EY-02660 (E.N. Pugh Jr.) and EY-12008 (J. Lem). E. N. Pugh Jr. is supported by a Jules & Doris Stein Research to Prevent Blindness Professorship.

Olaf S. Andersen served as editor.

Submitted: 10 January 2006
Accepted: 10 March 2006

REFERENCES

Applebury, M.L., M.P. Antoch, L.C. Baxter, L.L. Chun, J.D. Falk, F. Farhangfar, K. Kage, M.G. Krzystolik, L.A. Lyass, and J.T. Robbins. 2000. The murine cone photoreceptor: a single cone type expresses both S and M opsins with retinal spatial patterning. *Neuron.* 27:513–523.

Baylor, D.A., B.J. Nunn, and J.L. Schnapf. 1984. The photocurrent, noise and spectral sensitivity of rods of the monkey Macaca fascicularis. *J. Physiol.* 357:575–607.

Berntson, A., and W.R. Taylor. 2000. Response characteristics and receptive field widths of on-bipolar cells in the mouse retina. *J. Physiol.* 524(Pt 3):879–889.

Burkhardt, D.A. 1994. Light adaptation and photopigment bleaching in cone photoreceptors in situ in the retina of the turtle. *J. Neurosci.* 14:1091–1105.

Caenepeel, S., G. Charydczak, S. Sudarsanam, T. Hunter, and G. Manning. 2004. The mouse kinome: discovery and comparative genomics of all mouse protein kinases. *Proc. Natl. Acad. Sci. USA.* 101:11707–11712.

Calderone, J.B., and G.H. Jacobs. 1995. Regional variations in the relative sensitivity to UV light in the mouse retina. *Vis. Neurosci.* 12:463–468.

Calvert, P.D., N.V. Krasnoperova, A.L. Lyubarsky, T. Isayama, M. Nicolo, B. Kosaras, G. Wong, K.S. Gannon, R.F. Margolskee, R.L. Sidman, et al. 2000. Phototransduction in transgenic mice after targeted deletion of the rod transducin α-subunit. *Proc. Natl. Acad. Sci. USA.* 97:13913–13918 (published erratum appears in *Proc. Natl. Acad. Sci. USA.* 2000. 98:10515).

Carter-Dawson, L.D., and M.M. LaVail. 1979. Rods and cones in the mouse retina. I. Structural analysis using light and electron microscopy. *J. Comp. Neurol.* 188:245–262.

Chen, J., C.L. Makino, N.S. Peachey, D.A. Baylor, and M.I. Simon. 1995. Mechanisms of rhodopsin inactivation in vivo as revealed by a COOH-terminal truncation mutant. *Science.* 267(5196):374–377.

Chen, C.K., K. Zhang, J. Church-Kopish, W. Huang, H. Zhang, Y.J. Chen, J.M. Frederick, and W. Baehr. 2001. Characterization of human GRK7 as a potential cone opsin kinase. *Mol. Vis.* 7:305–313.

Cornwall, M.C., and G.L. Fain. 1994. Bleached pigment activates transduction in isolated rods of the salamander retina. *J. Physiol.* 480(Pt 2):261–279.

Cornwall, M.C., H.R. Matthews, R.K. Crouch, and G.L. Fain. 1995. Bleached pigment activates transduction in salamander cones. *J. Gen. Physiol.* 106:543–557.

Dacey, D.M. 1996. Circuitry for color coding in the primate retina. *Proc. Natl. Acad. Sci. USA.* 93:582–588.

Dacey, D.M. 2000. Parallel pathways for spectral coding in primate retina. *Annu. Rev. Neurosci.* 23:743–775.

Daniele, L.L., C. Lillo, A.L. Lyubarsky, S.S. Nikonov, N. Philp, A.J. Mears, A. Swaroop, D.S. Williams, and E.N. Pugh Jr. 2005. Cone-like morphological, molecular, and electrophysiological features of the photoreceptors of the *Nrl* knockout mouse. *Invest. Ophthalmol. Vis. Sci.* 46:2156–2167.

Engel, S.A., G.H. Glover, and B.A. Wandell. 1997. Retinotopic organization in human visual cortex and the spatial precision of functional MRI. *Cereb. Cortex.* 7:181–192.

Fei, Y., and T.E. Hughes. 2001. Transgenic expression of the jellyfish green fluorescent protein in the cone photoreceptors of the mouse. *Vis. Neurosci.* 18:615–623.

Frings, S., N. Brull, C. Dzeja, A. Angele, V. Hagen, U.B. Kaupp, and A. Baumann. 1998. Characterization of ether-a-go-go channels present in photoreceptors reveals similarity to IKx, a K^+ current in rod inner segments. *J. Gen. Physiol.* 111:583–599.

Ghosh, K.K., S. Bujan, S. Haverkamp, A. Feigenspan, and H. Wassle. 2004. Types of bipolar cells in the mouse retina. *J. Comp. Neurol.* 469:70–82.

Gillespie, P.G., and J.A. Beavo. 1988. Characterization of a bovine cone photoreceptor phosphodiesterase purified by cyclic GMP-sepharose chromatography. *J. Biol. Chem.* 263:8133–8141.

Govardovskii, V.I., N. Fyhrquist, T. Reuter, D.G. Kuzmin, and K. Donner. 2000. In search of the visual pigment template. *Vis. Neurosci.* 17:509–528.

Hestrin, S. 1987. The properties and function of inward rectification in rod photoreceptors of the tiger salamander. *J. Physiol.* 390:319–333.

Jacobs, G.H., J. Neitz, and J.F. Deegan. 1991. Retinal receptors in rodents maximally sensitive to ultraviolet light. *Nature.* 353:655–656.

Jeon, C.J., E. Strettoi, and R.H. Masland. 1998. The major cell populations of the mouse retina. *J. Neurosci.* 18:8936–8946.

Kenkre, J.S., N.A. Moran, T.D. Lamb, and O.A. Mahroo. 2005. Extremely rapid recovery of human cone circulating current at the extinction of bleaching exposures. *J. Physiol.* 567:95–112.

Klein, R., B.E. Klein, S.C. Tomany, S.M. Meuer, and G.H. Huang. 2002. Ten-year incidence and progression of age-related maculopathy: the beaver dam eye study. *Ophthalmology.* 109:1767–1779.

Lamb, T.D. 1981. The involvement of rod photoreceptors in dark adaptation. *Vision Res.* 21:1773–1782.

Lamb, T.D. 1995. Photoreceptor spectral sensitivities: common shape in the long-wavelength region. *Vision Res.* 35:3083–3091.

Lamb, T.D., and E.N. Pugh Jr. 1992. A quantitative account of the activation steps involved in phototransduction in amphibian photoreceptors. *J. Physiol.* 449:719–758.

Lerea, C.L., A.H. Bunt-Milam, and J.B. Hurley. 1989. α-Transducin is present in blue-, green-, and red-sensitive cone photoreceptors in the human retina. *Neuron.* 3:367–376.

Lerea, C.L., D.E. Somers, J.B. Hurley, I.B. Klock, and A.H. Bunt-Milam. 1986. Identification of specific transducin α subunits in retinal rod and cone photoreceptors. *Science.* 234:77–80.

Lukats, A., O. Dkhissi-Benyahya, Z. Szepessy, P. Rohlich, B. Vigh, N.C. Bennett, H.M. Cooper, and A. Szel. 2002. Visual pigment coexpression in all cones of two rodents, the Siberian hamster, and the pouched mouse. *Invest. Ophthalmol. Vis. Sci.* 43:2468–2473.

Lyubarsky, A.L., C. Chen, M.I. Simon, and E.N. Pugh Jr. 2000. Mice lacking G-protein receptor kinase 1 have profoundly slowed recovery of cone-driven retinal responses. *J. Neurosci.* 20:2209–2217.

Lyubarsky, A.L., B. Falsini, M.E. Pennesi, P. Valentini, and E.N. Pugh Jr. 1999. UV- and midwave-sensitive cone-driven retinal responses of the mouse: a possible phenotype for coexpression of cone photopigments. *J. Neurosci.* 19:442–455.

Lyubarsky, A.L., F. Naarendorp, X. Zhang, T. Wensel, M.I. Simon, and E.N. Pugh Jr. 2001. RGS9-1 is required for normal inactivation of mouse cone phototransduction. *Mol. Vis.* 7:71–78.

Lyubarsky, A.L., and E.N. Pugh Jr. 1996. Recovery phase of the murine rod photoresponse reconstructed from electroretinographic recordings. *J. Neurosci.* 16(2):563–571.

Matthews, H.R., M.C. Cornwall, and G.L. Fain. 1996. Persistent activation of transducin by bleached rhodopsin in salamander rods. *J. Gen. Physiol.* 108:557–563.

Mears, A.J., M. Kondo, P.K. Swain, Y. Takada, R.A. Bush, T.L. Saunders, P.A. Sieving, and A. Swaroop. 2001. Nrl is required for rod photoreceptor development. *Nat. Genet.* 29:447–452.

Nakatani, K., T. Tamura, and K.W. Yau. 1991. Light adaptation in retinal rods of the rabbit and two other nonprimate mammals. *J. Gen. Physiol.* 97:413–435.

Nikonov, S., N. Engheta, and E.N. Pugh Jr. 1998. Kinetics of recovery of the dark-adapted salamander rod photoresponse. *J. Gen. Physiol.* 111(1):7–37.

Nikonov, S., T.D. Lamb, and E.N. Pugh Jr. 2000. The role of steady phosphodiesterase activity in the kinetics and sensitivity of the light-adapted salamander rod photoresponse. *J. Gen. Physiol.* 116:795–824.

Nikonov, S.S., L.L. Daniele, X. Zhu, C.M. Craft, A. Swaroop, and E.N. Pugh Jr. 2005. Photoreceptors of *Nrl* $^{-/-}$ mice coexpress functional S- and M-cone opsins having distinct inactivation mechanisms. *J. Gen. Physiol.* 125:287–304.

Paupoo, A.A., O.A. Mahroo, C. Friedburg, and T.D. Lamb. 2000. Human cone photoreceptor responses measured by the electroretinogram a-wave during and after exposure to intense illumination. *J. Physiol.* 529(Pt 2):469–482.

Pennesi, M.E., J.H. Cho, Z. Yang, S.H. Wu, J. Zhang, S.M. Wu, and M.J. Tsai. 2003a. BETA2/NeuroD1 null mice: a new model for transcription factor-dependent photoreceptor degeneration. *J. Neurosci.* 23:453–461.

Pennesi, M.E., K.A. Howes, W. Baehr, and S.M. Wu. 2003b. Guanylate cyclase-activating protein (GCAP) 1 rescues cone recovery kinetics in GCAP1/GCAP2 knockout mice. *Proc. Natl. Acad. Sci. USA.* 100:6783–6788.

Pugh, E.N., Jr., and T.D. Lamb. 1993. Amplification and kinetics of the activation steps in phototransduction. *Biochim. Biophys. Acta.* 1141:111–149.

Pugh, E.N., Jr., S. Nikonov, and T.D. Lamb. 1999. Molecular mechanisms of vertebrate photoreceptor light adaptation. *Curr. Opin. Neurobiol.* 9:410–418.

Rebrik, T.I., and J.I. Korenbrot. 2004. In intact mammalian photoreceptors, Ca^{2+}-dependent modulation of cGMP-gated ion channels is detectable in cones but not in rods. *J. Gen. Physiol.* 123:63–75.

Robson, J.G., H. Maeda, S.M. Saszik, and L.J. Frishman. 2004. In vivo studies of signaling in rod pathways of the mouse using the electroretinogram. *Vision Res.* 44:3253–3268.

Rohlich, P., T. van Veen, and A. Szel. 1994. Two different visual pigments in one retinal cone cell. *Neuron.* 13:1159–1166.

Schnapf, J.L., B.J. Nunn, M. Meister, and D.A. Baylor. 1990. Visual transduction in cones of the monkey Macaca fascicularis. *J. Physiol.* 427:681–713.

Smith, N.P., and T.D. Lamb. 1997. The a-wave of the human electroretinogram recorded with a minimally invasive technique. *Vision Res.* 37:2943–2952.

Weiss, E.R., M.H. Ducceschi, T.J. Horner, A. Li, C.M. Craft, and S. Osawa. 2001. Species-specific differences in expression of G-protein-coupled receptor kinase (GRK) 7 and GRK1 in mammalian cone photoreceptor cells: implications for cone cell phototransduction. *J. Neurosci.* 21:9175–9184.

Wilkie, T.M., Y. Chen, D.J. Gilbert, K.J. Moore, L. Yu, M.I. Simon, N.G. Copeland, and N.A. Jenkins. 1993. Identification, chromosomal location, and genome organization of mammalian G-protein-coupled receptors. *Genomics.* 18:175–184.

Xu, J., R.L. Dodd, C.L. Makino, M.I. Simon, D.A. Baylor, and J. Chen. 1997. Prolonged photoresponses in transgenic mouse rods lacking arrestin. *Nature.* 389:505–509.

Ying, S., S.L. Fong, W.B. Fong, C.W. Kao, R.L. Converse, and W.W. Kao. 1998. A CAT reporter construct containing 277bp GNAT2 promoter and 214bp IRBP enhancer is specifically expressed by cone photoreceptor cells in transgenic mice. *Curr. Eye Res.* 17:777–782.

Yokoyama, R., and S. Yokoyama. 2000. Comparative molecular biology of visual pigments. *In* Molecular Mechanisms in Visual Transduction. D.G. Stavenga, W.J. de Grip, and E.N. Pugh Jr., editors. Elsevier Science Publishing Co., Inc., New York. 257–296.

Yoshida, S., A.J. Mears, J.S. Friedman, T. Carter, S. He, E. Oh, Y. Jing, R. Farjo, G. Fleury, C. Barlow, et al. 2004. Expression profiling of the developing and mature *Nrl*$^{-/-}$ mouse retina: identification of retinal disease candidates and transcriptional regulatory targets of Nrl. *Hum. Mol. Genet.* 13:1487–1503.

Zhang, X., T.G. Wensel, and T.W. Kraft. 2003. GTPase regulators and photoresponses in cones of the eastern chipmunk. *J. Neurosci.* 23:1287–1297.